# Copper Binding to the Neurotoxic Peptide $PrP_{106–126}$: Thermodynamic and Structural Studies

Barbara Belosi,[a] Elena Gaggelli,[b] Remo Guerrini,[c] Henryk Kozłowski,*[d] Marek Łuczkowski,[d] Francesca M. Mancini,[b] Maurizio Remelli,*[a] Daniela Valensin,[b] and Gianni Valensin[b]

*The human prion protein fragment $PrP_{106–126}$ is a highly fibrillogenic peptide, resistant to proteinases and toxic to neurons; it derives from the normal prion protein ($PrP^C$), with which it can interact, thus inhibiting its superoxide dismutase-like activity. The same properties are also shown by the abnormal isoform of the prion protein ($PrP^{Sc}$), and this similarity makes $PrP_{106–126}$ an interesting model for the neurotoxic action of $PrP^{Sc}$. A role for copper in $PrP_{106–126}$ aggregation and toxicity has recently been evidenced, and the interaction of terminal Lys, His and Met residues with the copper ion at neutral pH has been suggested.*

*In order to shed more light on the complex-formation equilibria of $PrP_{106–126}$ with the copper ion, a thorough investigation has been carried out by means of several experimental techniques: potentiometry, solution calorimetry, VIS spectrophotometry, circular dichroism, EPR and NMR spectroscopy. A shorter and more soluble fragment—$PrP_{106–113}$, which lacks the hydrophobic C-terminal domain of $PrP_{106–126}$ but contains all the potential donor groups—has also been considered for the sake of comparison. The involvement of terminal amino, imidazolic and amido nitrogens in complex formation has been confirmed, while no evidence was found for the interaction of side chains of Met and Lys residues with the copper ion. Solution structures for the main complexes are suggested.*

## Introduction

Neurodegenerative disorders have recently been recognised as a priority health problem in the most developed countries, mainly because of the increase in life expectancy. Besides the most common Alzheimer's and Parkinson's diseases, great concern also derives from the so-called "prion diseases" or spongiform encephalopathies.[1] They may be present as genetic, sporadic, or even infectious disorders, and it has been accepted that they can be transmitted from animals to humans.[2] They include scrapie in sheep, bovine spongiform encephalopathy (BSE) in cattle and Creutzfeldt – Jacob disease (CJD) in humans. Prions are infectious pathogens, devoid of nucleic acid, which seem to be composed exclusively of a modified isoform of a protein, namely the prion protein (PrP), designated $PrP^{Sc}$. The normal PrP ($PrP^C$) is converted into $PrP^{Sc}$ through a process which does not involve any change in its primary structure: a portion of its $\alpha$-helical and coil structure is refolded into a $\beta$-sheet.[2] This structural transition is accompanied by profound changes in its physicochemical properties: $PrP^C$ is soluble in non-denaturing detergents whereas $PrP^{Sc}$ is not, $PrP^C$ is digested by proteases whereas $PrP^{Sc}$ is partially resistant, and $PrP^{Sc}$ readily aggregates into amyloid fibrils. As a consequence, $PrP^{Sc}$ accumulates in the brain and also in other organs. Although the normal functions of $PrP^C$ are not yet completely understood[3] it is known that the prion protein can bind $Cu^{II}$ ions in vivo,[4] and a fundamental role of $PrP^C$ in copper metabolism has been suggested.[5] Moreover, the $Cu^{II}$ ion has been recognised as a co-factor for the protein refolding.[6, 7] Copper interaction with the full-length recombinant PrP and many of its fragments has been the subject of several research papers.[8]

Increasing interest has in recent years been devoted to the peptide fragment $PrP_{106–126}$, encompassing residues 106 – 126 of human PrP (see Scheme 1). $PrP_{106–126}$ has been shown to be highly fibrillogenic, resistant to proteinase K and toxic to neurones in vitro[9, 10] and in vivo;[11] however, expression of $PrP^C$ is required for $PrP_{106–126}$ neurotoxicity[12] exactly as in the case of $PrP^{Sc}$.[13] In addition, it has been shown that both $PrP^{Sc}$ and $PrP_{106–126}$ can interact with recombinant $PrP^C$ in the same region, namely the hydrophobic region 112 – 119, inhibiting the super-

[a] *Dr. B. Belosi, Prof. M. Remelli*
*Dipartimento di Chimica, Università di Ferrara*
*via L. Borsari 46, 44100 Ferrara (Italy)*
*Fax: (+39) 0532-240709*
*E-mail: rmm@unife.it*

[b] *Prof. E. Gaggelli, Dr. F. M. Mancini, Dr. D. Valensin, Prof. G. Valensin*
*Dipartimento di Chimica, Università di Siena*
*via A. Moro, S. Miniato, 53100 Siena (Italy)*

[c] *Dr. R. Guerrini*
*Dipartimento of Scienze Farmaceutiche, Università di Ferrara*
*via Fossato di Mortara 17/19, 44100 Ferrara (Italy)*

[d] *Prof. H. Kozłowski, Dr. M. Łuczkowski*
*Faculty of Chemistry, University of Wrocław*
*F. Joliot-Curie 14, 50 – 383 Wrocław (Poland)*
*Fax: (+48) 71-3757251*
*E-mail: henrykoz@wchuwr.chem.uni.wroc.pl*

*Supporting information for this article is available on the WWW under http://www.chembiochem.org or from the author.*

 **DOI: 10.1002/cbic.200300786**  

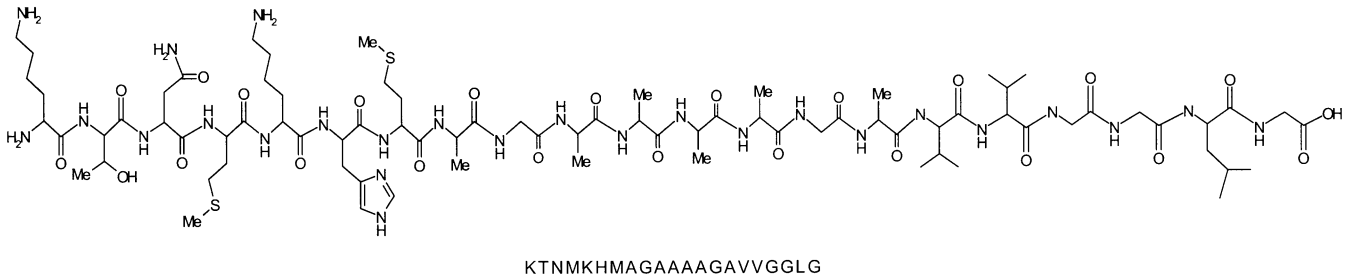


***Scheme 1.*** *The neurotoxic peptide fragment $PrP_{106-126}$.*

oxide dismutase-like activity of $PrP^{C}$.[12] All these properties make $PrP_{106-126}$ an interesting model for the neurotoxic action of $PrP^{Sc}$.[14] A role for copper in $PrP_{106-126}$ aggregation and toxicity has also been suggested,[12] as in the case of prion protein or Alzheimer's disease amyloid β peptide.[15] The interaction between copper and $PrP_{106-126}$ at physiological pH was recently studied by Jobling et al.[16] They found that $PrP_{106-126}$ aggregation can be first drastically abolished by reducing the copper and zinc levels in Chelex-100-treated buffer and then restored if the copper and zinc levels are restored to their original values. From EPR and NMR data on $Cu^{II}/PrP_{106-126}$ solution and from parallel investigations on some peptide analogues they suggested 2 N 1 S 1 O coordination to the copper ion, involving the terminal amino group, the $His_{111}$ residue imidazole, a sulfur atom—most probably belonging to the Met112 residue of a second polypeptide chain—and an oxygen that could derive either from a carbonyl group of the peptide backbone or from a water molecule. They confirmed that $Cu^{II}$ and/or $Zn^{II}$ binding is critical for $PrP_{106-126}$ toxicity, as also reported in other investigations on the peptide's ability to generate hydroxyl radicals.[17, 18]

In order to shed more light on the copper-binding ability of the $PrP_{106-126}$ peptide, in this paper the $Cu^{II}$ complex-formation equilibria of $PrP_{106-126}$ and the shorter $PrP_{106-113}$ fragment protected at its carboxylic end (KTNMKHMA-$NH_2$) have been investigated in aqueous solution and over a wide pH range, at $I = 0.1$ M and $T = 298.2$ K. $PrP_{106-113}$ shares its amino-terminal domain, containing the most important donor atoms, with the neurotoxic peptide $PrP_{106-126}$, while it lacks the hydrophobic core (residues 114–126) responsible for peptide aggregation.[19] Protonation and complex-formation constants were potentiometrically determined, formation enthalpies were measured by direct solution calorimetry, and the complex-formation model and species stoichiometry were carefully checked by UV/Vis absorption, CD, EPR and NMR spectroscopy. Structure hypotheses on the main complex species are suggested.

## Results

Thermodynamic results on protonation equilibria are reported in Tables 1 and 2; they are in good agreement with previous results on similar systems.[20]

Protonation constant values are almost the same for the two ligands, confirming that the presence of the carboxy-terminal hydrophobic chain of $PrP_{106-126}$ does not influence its acid–base behaviour. The most basic sites of both the ligands are the side amino groups of Lys106 and Lys110 residues. The first log $K$ value is close to that of lysine itself (10.68),[21] while the second is lower, for enthalpic reasons (see Table 1). The available data do not make it possible to recognise which of the two Lys residues bears the more basic side chain. The third protonation should be due to the terminal amino group and the fourth to the imidazole side chain of His111. Finally, $PrP_{106-126}$ bears an unprotected carboxylic group, the log $K$ value of which is very close to that reported for oligopeptides with a C-terminal aliphatic chain.[21]

Table 3 shows the thermodynamic parameters of complex formation between the $Cu^{II}$ ion and $PrP_{106-113}$; a representative species-distribution diagram is shown in Figure 1. Table 4 reports the spectroscopic parameters, and some experimental spectra are shown in the Supporting Information.

***Table 1.*** *Thermodynamic parameters for $PrP_{106-113}$ protonation.*

| Species | log β | log $K_{step}$ | $-\Delta G^{\circ}$ [kJ mol$^{-1}$] | $-\Delta H^{\circ}$ [kJ mol$^{-1}$] | $\Delta S^{\circ}$ [J mol$^{-1}$ K$^{-1}$] |
|---|---|---|---|---|---|
| LH | 10.50 (1) | 10.50 | 59.9 (1) | 67 (1) | −24 (5) |
| $LH_2$ | 20.43 (1) | 9.93 | 116.5 (1) | 112 (1) | 15 (4) |
| $LH_3$ | 27.63 (1) | 7.20 | 157.6 (1) | 154 (1) | 11 (4) |
| $LH_4$ | 33.68 (1) | 6.05 | 192.2 (1) | 181 (1) | 38 (4) |

***Table 2.*** *Protonation constants for $PrP_{106-126}$.*

| Species | log β | log $K_{step}$ |
|---|---|---|
| LH | 10.54 (1) | 10.54 |
| $LH_2$ | 20.36 (1) | 9.82 |
| $LH_3$ | 27.63 (2) | 7.27 |
| $LH_4$ | 33.62 (2) | 5.99 |
| $LH_5$ | 37.04 (2) | 3.42 |

***Table 3.*** *Thermodynamic parameters for the system $Cu^{II}/PrP_{106-113}$.*

| Species | log β | log $K_{step}$ | $-\Delta G^{\circ}$ [kJ mol$^{-1}$] | $-\Delta H^{\circ}$ [kJ mol$^{-1}$] | $\Delta S^{\circ}$ [J mol$^{-1}$ K$^{-1}$] |
|---|---|---|---|---|---|
| $MLH_3$ | 30.8 (1) | | 175.7 (5) | n.d.[a] | n.d. |
| $MLH_2$ | 26.73 (1) | 4.1 | 152.4 (1) | 166 (3) | −45 (10) |
| MLH | 22.17 (1) | 4.56 | 126.5 (1) | 126 (1) | 1 (4) |
| ML | 15.61(2) | 6.56 | 89.1 (1) | 99 (1) | −32 (4) |
| $MLH_{-1}$ | 7.33 (2) | 8.28 | 41.8 (1) | 55 (1) | −43 (4) |
| $MLH_{-2}$ | −2.53 (3) | 9.86 | −14.4 (1) | 19 (2) | −112 (6) |
| $MLH_{-3}$ | −13.12 (3) | 10.59 | −74.8 (1) | −47 (2) | −98 (7) |
| $MLH_{-4}$ | −24.74 (8) | 11.62 | −141.1 (2) | n.d. | n.d. |

[a] n.d. = not determined.

  

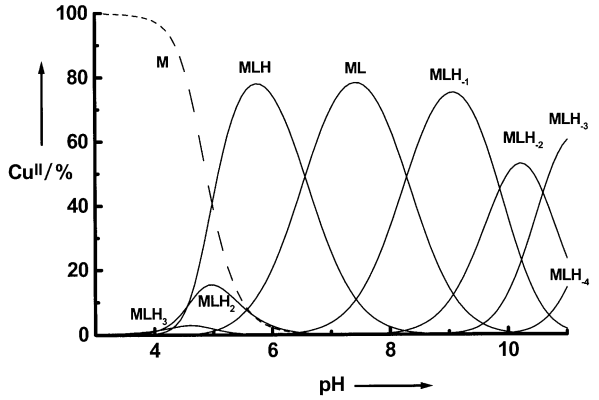


***Figure 1.*** *Distribution diagram for the system $Cu^{II}/PrP_{106-113}$. $[Cu^{II}] = [PrP_{106-113}] = 1.0$ mM.*

***Table 4.*** *Spectroscopic results for the $Cu^{II}/PrP_{106-113}$ system.*

| pH | Main species | VIS absorption | | CD | | EPR | |
|---|---|---|---|---|---|---|---|
| | | $\lambda$ [nm] | $\varepsilon$ [$M^{-1}cm^{-1}$] | $\lambda$ [nm] | $\Delta\varepsilon$ [$M^{-1}cm^{-1}$] | $A_{\parallel}$ | $g_{\parallel}$ |
| 4.0 | $MLH_3$, $MLH_2$ | 792 | 15 | 263 | 0.09 | 121 | 2.41 |
| 5.0 | $MLH_2$, MLH | 620 | 58 | 619 | −0.44 | 163 | 2.22 |
| | | | | 317 | 0.48 | | |
| | | | | 274 | −0.76 | | |
| | | | | 235 | −2.13 | | |
| 6.0 | MLH | 601 | 114 | 607 | −0.75 | 163 | 2.22 |
| | | | | 316 | 0.89 | | |
| | | | | 275 | −1.53 | | |
| | | | | 241 | −2.98 | | |
| 7.5 | ML | 559 | 148 | 582 | −1.03 | 182 | 2.21 |
| | | | | 487 | 0.25 | | |
| | | | | 316 | 1.43 | | |
| | | | | 278 | −2.91 | | |
| | | | | 248 | 2.23 | | |
| 9.0 | $MLH_{-1}$ | 539 | 156 | 564 | 1.32 | 195 | 2.20 |
| | | | | 479 | 0.28 | | |
| | | | | 312 | 1.46 | | |
| | | | | 274 | −3.18 | | |
| | | | | 249 | 2.4 | | |
| 10.0 | $MLH_{-2}$ | 522 | 156 | 560 | −1.48 | 192 | 2.20 |
| | | | | 477 | 0.28 | | |
| | | | | 309 | 1.58 | | |
| | | | | 274 | −3.63 | | |
| | | | | 251 | 1.25 | | |
| 11.0 | $MLH_{-3}$ | 520 | 163 | 558 | −1.56 | 197 | 2.20 |
| | | | | 473 | 0.23 | | |
| | | | | 309 | 1.55 | | |
| | | | | 273 | −3.85 | | |
| | | | | 250 | 1.64 | | |
| 12.0 | $MLH_{-4}$ | n.d.[a] | n.d. | 555 | −1.61 | 202 | 2.17 |
| | | | | 472 | 0.2 | | |
| | | | | 310 | 1.6 | | |
| | | | | 272 | −4.14 | | |
| | | | | 250 | 1.58 | | |

[a] n.d. = not determined.

$PrP_{106-113}$ begins to bind the metal ion below pH 4: the wavelength of maximum absorption at that pH value is 780 nm, significantly lower than the expected value for the hexa-aquo $Cu^{II}$ ion. When pH is increased, a regular "blue-shift" is registered; this suggests the coordination of an increasing number of nitrogen atoms. The distribution diagram shows that three species form at the lowest pH values, that is, the $MLH_3$, $MLH_2$ and MLH complexes, the last of these being the most important species in the acidic pH range. At pH 5, the ML complex appears: it dominates at physiological pH values. In the alkaline pH range, the complex undergoes some further deprotonation steps, leading to the formation of $MLH_{-1}$, $MLH_{-2}$, $MLH_{-3}$ and $MLH_{-4}$ complexes. The CD spectra show some typical absorption bands:[22] a double band characteristic of $Cu^{II}$/His coordination in the d – d region, a positive band—most probably due to a c.t. (charge transfer) transition from a deprotonated amido nitrogen to copper—at 310 – 320 nm, a negative band attributable to a c.t. transition from imidazole to copper at 275 nm, and a positive band attributable to a c.t. transition from terminal amino group to the metal ion at 235 – 250 nm. The $A_{\parallel}$ and $g_{\parallel}$ parameters of the EPR spectra are reported in Table 4: they show the existence of three major species.[23] No evidence of binuclear species was found throughout the whole pH range.

Complex-formation constants for the $Cu^{II}/PrP_{106-126}$ system are reported in Table 5, while Figure 2 shows the corresponding distribution diagram. Some EPR spectra are reported in the Supporting Information, and CD spectra at variable pH values are shown in Figure 3. All the spectroscopic results are collected in Table 6. Comparison of such results with those relating to the shorter $PrP_{106-113}$ fragment suggests that the two systems behave in a nearly identical way: the stoichiometries of the formed complexes are the same and the corresponding constant

***Table 5.*** *Complex formation constants for the $Cu^{II}/PrP_{106-126}$ system.*

| Species | $\log\beta$ | $\log K_{step}$ |
|---|---|---|
| $MLH_3$ | 31.5 (2) | |
| $MLH_2$ | 26.8 (1) | 4.7 |
| MLH | 22.04 (5) | 4.8 |
| ML | 15.12(9) | 6.9 |
| $MLH_{-1}$ | 6.55 (1) | 8.6 |
| $MLH_{-2}$ | −3.2 (1) | 9.7 |
| $MLH_{-3}$ | −13.9 (2) | 10.7 |
| $MLH_{-4}$ | −25.3 (3) | 11.4 |

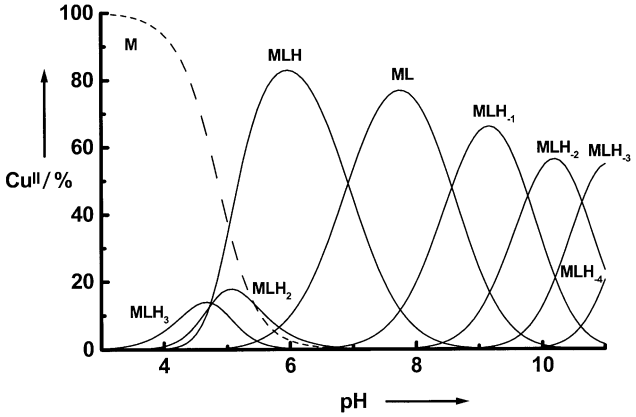


***Figure 2.*** *Distribution diagram for the $Cu^{II}/PrP_{106-126}$ system. $[Cu^{II}] = [PrP_{106-126}] = 1.0$ mM.*

  

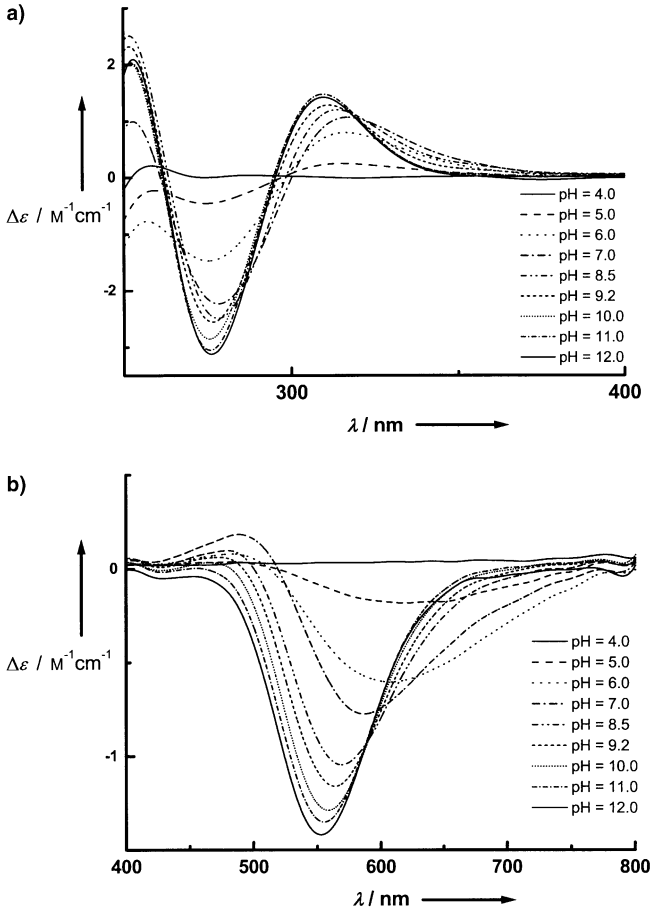


*Figure 3. CD spectra for the $Cu^{II}/PrP_{106-126}$ system. $[Cu^{II}] = [PrP_{106-126}] = 1.0$ mM. a) Charge-transfer transitions; b) d – d transitions.*

*Table 6. Spectroscopic results for the $Cu^{II}/PrP_{106-126}$ system.*

| pH | Main species | Vis absorption | | CD | | EPR | |
|---|---|---|---|---|---|---|---|
| | | λ [nm] | ε [M⁻¹ cm⁻¹] | λ [nm] | Δε [M⁻¹ cm⁻¹] | $A_{\parallel}$ | $g_{\parallel}$ |
| 4.0 | $MLH_3$ | n.d.[a] | n.d. | 258 | 0.21 | 121 | 2.41 |
| 5.0 | $MLH_3$ | 637 | 48 | 619 | −0.18 | 174 | 2.22 |
| | $MLH_2$, MLH | | | 315 | 0.25 | | |
| | | | | 274 | −0.46 | | |
| 6.0 | MLH | 619 | 99 | 607 | −0.60 | 177 | 2.22 |
| | | | | 316 | 0.80 | | |
| | | | | 275 | −1.47 | | |
| 7.8 | ML | 561 | 124 | 578 | −0.91 | 195 | 2.20 |
| | | | | 315 | 1.14 | | |
| | | | | 278 | −2.31 | | |
| | | | | 252 | 1.75 | | |
| 9.2 | $MLH_{-1}$ | 539 | 129 | 564 | −1.16 | 195 | 2.19 |
| | | | | 311 | 1.28 | | |
| | | | | 276 | −2.56 | | |
| | | | | 252 | 2.32 | | |
| 10.0 | $MLH_{-2}$ | 520 | n.d. | 558 | −1.29 | 202 | 2.19 |
| | | | | 310 | 1.42 | | |
| | | | | 275 | −2.86 | | |
| | | | | 252 | 2.04 | | |
| 11.0 | $MLH_{-3}$ | 522 | n.d. | 555 | −1.35 | 200 | 2.19 |
| | | | | 310 | 1.48 | | |
| | | | | 276 | −3.05 | | |
| | | | | 252 | 2.03 | | |
| 12.0 | $MLH_{-4}$ | n.d. | n.d. | 553 | −1.42 | 200 | 2.18 |
| | | | | 310 | 1.42 | | |
| | | | | 276 | −3.12 | | |
| | | | | 253 | 2.09 | | |

[a] n.d. = not determined.

values are rather close to each other. The spectroscopic data are very similar as well. These results suggest that both the hydrophobic tail and the terminal carboxylic group of $PrP_{106-126}$ play secondary roles in the $Cu^{II}$ complex formation. Note, all discussion on the suggested structures for the complex species is for the two ligands together.

The NMR investigation on the $Cu^{II}$ complexes was performed only for the shortest $PrP_{106-113}$ fragment at pH 5.6, 7.4 and 9.0, at which the predominance of MHL, ML and $MLH_{-1}$, respectively, was shown by equilibrium studies. The $^1H$ NMR spectrum of $PrP_{106-113}$ in $H_2O/D_2O$ at pH 5.6 is shown in Figure 4 (lower traces), and the assignments are reported in Table 7. As previously observed,[16] the peptide is completely unfolded in solution (no significant NOESY or ROESY cross-peaks could be detected) and, as would be expected from the lacking hydrophobic domain, no aggregation was monitored up to the concentration of 3.2 mM. When the pH was raised, the amide protons underwent rapid chemical exchange with the solvent, resulting in extensive line broadening, as usually observed for short peptides.[24, 25] For this reason, NMR spectra at pH 7.4 and 9.0 were obtained from peptide solutions in $D_2O$. The assignment at pH 7.4 is also reported in Table 7.

Titration with increasing amounts of $Cu(NO_3)_2$ resulted in some selective line broadening in the NMR spectrum, as shown in Figure 4 (upper traces) for a peptide/$Cu^{II}$ ratio of 10:1. The paramagnetic effect, however, is much less pronounced than expected and even at the ratio of 2.5:1, only a few resonances—namely, the imidazole protons of His111—were broadened beyond detection. Similar findings have been obtained with copper interacting with other histidine-containing peptides;[26, 27] the imidazole ring of histidine behaves as a strong anchoring site for $Cu^{II}$, which results in large stability constants and, as a consequence, in relatively slow off-rates $k_{off}$. This being the case, the residence lifetime of the metal at its binding site makes a contribution to the paramagnetic relaxation rate which cannot be neglected.

$$R_{ip} = R_{iobs} - \frac{p_f}{R_{if}^{-1}} = \frac{p_b}{R_{ib}^{-1} + k_{off}^{-1}} \quad [i = 1,2] \tag{1}$$

Here $p_b$ and $p_f$ are the fractional populations of the peptide in the metal-bound state and in the bulk solution, respectively, and $R_{ib}$ and $R_{if}$ are the relaxation rates in the two environments. In such a situation, the closer a proton is to the paramagnetic ion, the faster is $R_{ib}$ and, therefore, the more important becomes the contribution of $k_{off}^{-1}$ to $R_{iobs}$. It follows that $k_{off}$ must be determined whenever the structure of the complex is sought by measuring the paramagnetic contribution to the nuclear spin-lattice relaxation rate $R_1$, which reflects the dipolar interaction energy (proportional to the inverse sixth power of the metal – proton distance) between the electron and nuclear spin.

  

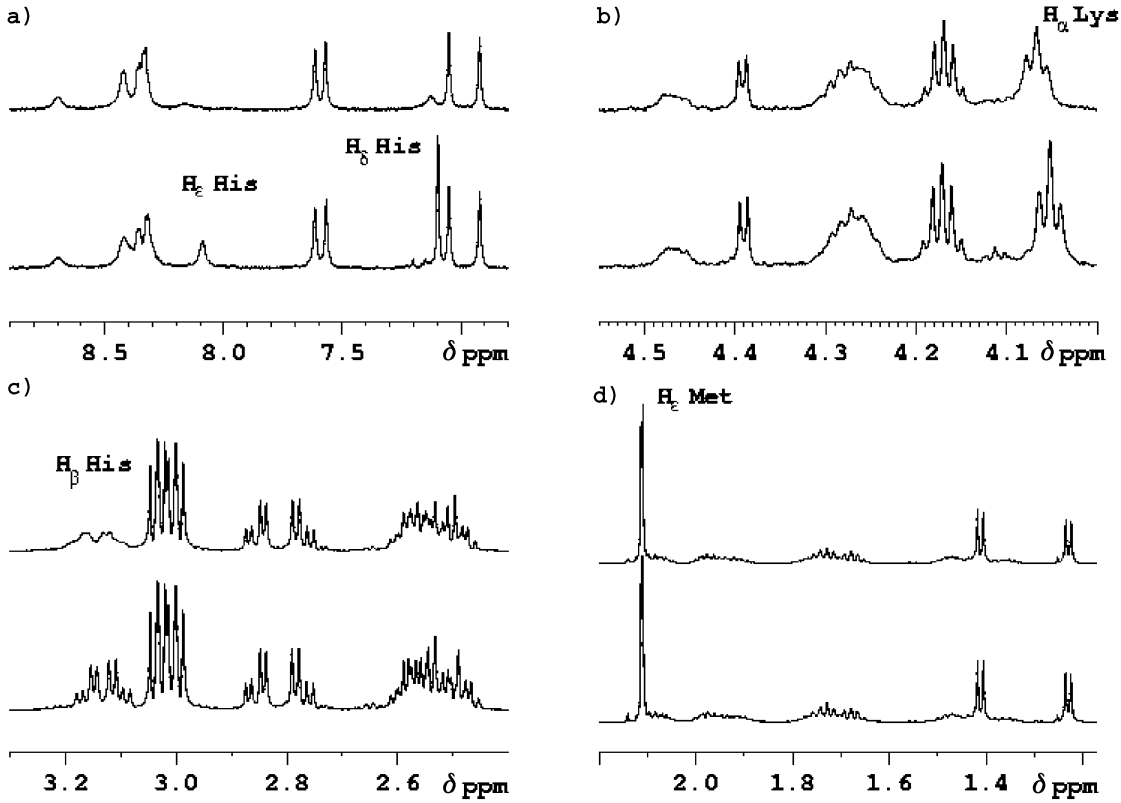


***Figure 4.*** *Selected regions of the $^1$H NMR spectra of $PrP_{106–113}$ (1.6 mM in $D_2O/H_2O$ at pH 5.6) before (lower traces) and after (upper traces) the addition of $Cu^{II}$ (0.16 mM): a) amide and aromatic region; b) $H_\alpha$ region; c) 2.3 – 3.3 ppm region, d) 1.2 – 2.2 ppm region.*

***Table 7.*** *$^1$H NMR chemical shifts [ppm] of $PrP_{106–113}$ [2 mM] at $T = 298$ K.*

| | HN | Hα | Hβ | Hγ | Others |
|---|---|---|---|---|---|
| **pH 5.6** | | | | | |
| Lys106 | | 4.11 | 1.95 – 1.73 | 1.48 | $H_\varepsilon$ 3.03 |
| Thr107 | | 4.39 | 4.16 | 1.23 | |
| Asn108 | 8.68 | 4.75 | 2.86 – 2.78 | | $NH_{sc}$ 7.60 – 6.91 |
| Met109 | 8.43 | 4.47 | 2.09 – 1.98 | 2.53 – 2.58 | $H_\varepsilon$ 2.11 |
| Lys110 | 8.33 | 4.26 | 1.76 – 1.71 | 1.41 | $H_\varepsilon$ 3.01 |
| His111 | 8.53 | 4.67 | 3.25 – 3.17 | | $H_\varepsilon$ 8.53, $H_\delta$ 7.26 |
| Met112 | 8.41 | 4.47 | 2.09 – 1.98 | 2.53 – 2.58 | $H_\varepsilon$ 2.11 |
| Ala113 | 8.37 | 4.28 | 1.42 | | |
| $NH_2$ amide | 7.57 – 7.03 | | | | |
| **pH 7.4** | | | | | |
| Lys106 | | | 1.73 | 1.45 – 1.37 | $H_\varepsilon$ 3.01 |
| Thr107 | | 4.36 | 4.20 | 1.24 | |
| Asn108 | | 4.74 | 2.86 – 2.79 | | |
| Met109 | | 4.48 | 2.09 – 1.99 | 2.53 – 2.58 | $H_\varepsilon$ 2.12 |
| Lys110 | | 4.26 | 1.81 | 1.73 | $H_\varepsilon$ 3.01 |
| His111 | | 4.61 | 3.09 | | $H_\varepsilon$ 7.75, $H_\delta$ 6.98 |
| Met112 | | 4.46 | 2.08 – 1.99 | 2.53 – 2.45 | $H_\varepsilon$ 2.12 |
| Ala113 | | 4.29 | 1.42 | | |

The measured paramagnetic relaxation enhancements, $R_{1p}$ values, are summarized in Figure 5. From a qualitative point of view the following is observed:

i) the paramagnetic effects on the imidazole protons of His111 are the largest at any pH value,
ii) Hα of Lys106 and Hβ of His111 are also somehow affected, especially at pH 5.6,
iii) quite unexpectedly, paramagnetic contributions to most, but not all, protons are consistently lowered by raising the pH, and
iv) in contrast to the previous observation, some protons are more affected at pH 9.0 than pH 7.4.

Again, all these observations ratify the role played by $k_{off}$ in determining $R_{1p}$: raising the pH produces a change in stability constants and consequently increases the size of the exchange contribution to $R_{1p}$.

The exchange rates were measured in two different ways. The temperature dependence of $R_{1p}$ is the commonly exploited method for measuring $k_{off}$, by fitting of the negative slope of $\ln R_{1p}$ against $^1/_T$ curves to the Eyring equation:[28]

$$k_{off} = \frac{kT}{h} e^{-\frac{\Delta G^\#}{RT}}$$

$$\ln [R_{1p}] = \ln \left[ p_b \frac{kT}{h} \right] \frac{\Delta G^\#}{RT} \quad (2)$$

Here $\Delta G^\#$ is the free energy of activation for the dissociation process. A typical plot for the imidazole protons of His111 at pH 7.4 is shown in Figure 6. Such measurements are often impaired by flattened temperature dependencies arising from intermediate exchange conditions or in cases where the paramagnetic effects are relatively small. For this reason an alternative and equivalent method taking advantage of $H_\varepsilon$ of $Cu^{II}$-bound histidine being at a fixed distance of 0.31 nm from the paramagnetic centre was devised.[29] The $R_{1p}$ of the $H_\varepsilon$ can

  

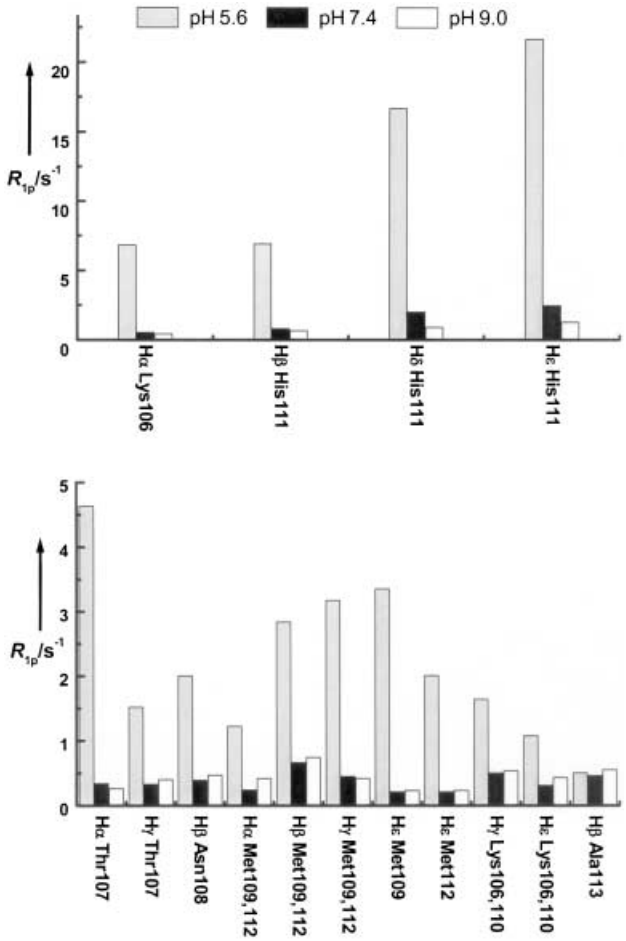


***Figure 5.*** *$R_{1p}$ values measured for selected protons in $PrP_{106-113}$ (1.6 mM in $D_2O$/$H_2O$ at pH 5.6) after the addition of $Cu^{II}$ (0.32 mM).*

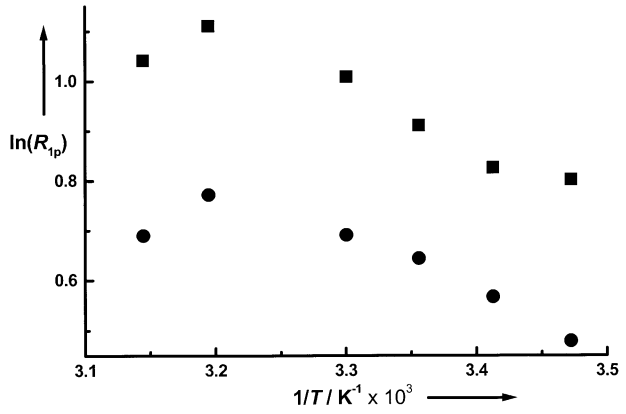


***Figure 6.*** *Temperature dependence of the $R_{1p}$ values measured for selected protons in $PrP_{106-113}$ (2.0 mM in $D_2O/H_2O$ at pH 7.4) after the addition of $Cu^{II}$ (0.4 mM). ■ = $H_\varepsilon$ His111 ● = $H_\delta$ His111.*

therefore be immediately considered for evaluation of $k_{off}^{im}$ (imidazole). It is worth underlining that in both the present and in other cases, the two methods provide $k_{off}^{im}$ values in very good agreement with each other. The values calculated for the imidazole protons of His111 at the three pH values are reported in Table 8. As anticipated, $k_{off}$ becomes slower and slower at increasing pH, such that at pH > 7.4 $R_{1p}$ is almost determined by $k_{off}^{-1}$.

***Table 8.*** *Off-rate values for backbone ($k_{off}^{-1(bb)}$) and imidazole ($k_{off}^{-1(im)}$) protons of the $PrP_{106-113}$-$Cu^{II}$ complex, at T = 298 K.*

| | $k_{off}^{-1(im)}$ [s] | $k_{off}^{-1(bb)}$ [s][a] |
|---|---|---|
| pH 5.6 | 0.009 | 0.029 |
| pH 7.4 | 0.080 | 0.345 |
| pH 9.0 | 0.154 | 0.435 |

[a] Use of only the lowest and highest values of the distance range results in a very small error (±0.001 s).

The exchange rate calculated for the imidazole ring is not likely to apply to backbone protons, since binding would be expected to occur as a multistep process starting with the entrance of the anchoring site into the metal coordination sphere. That this is the case is further supported by the observation that some selected backbone or side chain protons experienced relatively large paramagnetic effects that would, however, result in exceedingly long distances, should the same exchange rate hold for all protons. An estimate of $k_{off}^{bb}$ (backbone) was therefore obtained by considering that binding to the N-terminal amino group should result in Hα of Lys106 being located at distances from $Cu^{II}$ in the range from 0.23 – 0.40 nm. As a consequence, the $R_{1p}$ of the same proton is consistent with the $k_{off}^{bb}$ rates also reported in Table 8. The obtained exchange rates suggest that at neutral or basic pH the paramagnetic effects are almost exclusively determined by exchange such that metal – proton distances cannot be calculated.

## Discussion

The species which forms at the most acidic pH (≤ 4) is the complex $MLH_3$. Its stoichiometry suggests that the ligand is triprotonated while the fourth basic site is bound to the copper ion. The most basic sites are the side chain amino groups of Lys106 and Lys110 (see Tables 1 and 2): according to previous data on peptides also containing one or more lysine residues,[20, 26] they should be protonated. From the present data, it cannot be said whether the copper-promoted deprotonation takes place at the terminal amino group, as usually happens with unprotected peptides,[30] or at the imidazole nitrogen of His111 residue, as already reported with protected His-containing peptides.[20] Competition between the two donor sites is most probably operative, as found previously.[26] The two resulting structural hypotheses for the $MLH_3$ complex are presented in the Supporting Information. It is worth noting that the $\log\beta_{113}$ value relative to the $PrP_{106-126}$ ligand (Table 5) is higher than the corresponding value found for $PrP_{106-113}$ (Table 3) by about 0.7 $\log\beta$ units. A contribution from the terminal carboxylic group to the complex stability could not be excluded in the former case.

  

At a pH value just higher than 4, the species $MLH_2$ is formed. The corresponding $\log K_{step}$ value ($=\log\beta_{113}-\log\beta_{112}=4.1$) and the trend shown by the spectroscopic parameters (Table 4) support the hypothesis of coordination of both the terminal amine and imidazole nitrogen atoms to copper (see Supporting Information). Subtraction of the enthalpic contribution due to the protonated side chains of Lys residues from the $MLH_2$ formation enthalpy ($\Delta H^{\circ}_{112}-\Delta H^{\circ}_{012} = -166+112 = -54\,kJ\,mol^{-1}$) gives a computed value in excellent agreement with the literature value for the $[Cu(histamine)]^{2+}$ complex under the same experimental conditions ($-51\,kJ\,mol^{-1}$; ref. [31]). In the latter species the donor centres are just an amino and an imidazole group, as hypothesized for this $MLH_2$ species. A macrochelate ring should form in this case, as already previously reported in literature for an unprotected pentadecapeptide derived from the SPARC protein.[20]

The main species in the acidic pH range closest to neutrality is the complex MLH, which binds almost all the copper ion present in solution. A further "blue shift" is recorded in VIS spectra (see Supporting Information and Tables 4 and 6); this suggests the coordination of another nitrogen atom to the metal. Taking into account that the side amino group of Lys residues do not normally bind copper in this pH range,[20, 26, 32] the deprotonation of an amido nitrogen of a peptide bond and its coordination to the metal ion are suggested. This normally happens, from pH 5 onwards, with short peptides.[30] Comparison between the corresponding $pK_{step}$ ($=\log\beta_{112}-\log\beta_{111}=4.6$) and $\Delta H^{\circ}_{step}$ ($\Delta H^{\circ}_{112}-\Delta H^{\circ}_{111}=-40\,kJ\,mol^{-1}$) with averaged literature values[21] supports this hypothesis. CD spectra show all the expected signals for the suggested donor atom set (see Supporting Information, Figure 3, Tables 4 and 6). It is worth noting that the $N_{Im}$—$Cu^{II}$ bond is often characterized by a charge-transfer band located around 340 nm.[22, 32] Although it is not directly observable here as a well-defined absorption maximum, it should be responsible for the long tail shown by the intense band at 310–317 nm. This in turn can be ascribed to an amide $N^-$—$Cu^{II}$ bond.[22] The wavelength of maximum absorption found in the visible spectrum at pH 6.0 is 601 nm for the $Cu^{II}/PrP_{106-113}$ system and only slightly higher with $PrP_{106-126}$. These values are compatible with that computed from the Sigel–Martin empirical formula[33] (593 nm) concerning $Cu^{II}$ complexes with the suggested donor atom set {$NH_2$, $N_{im}$, $N^-$}. This is also in agreement with EPR results.[23] It is worth noting that the identification of the donor groups of the ligand does not unequivocally determine the complex structure. In fact, each amido nitrogen of the peptide backbone is theoretically available to bind the metal ion. The two most likely structural hypotheses are those in which the amido nitrogen bound to copper ion is that belonging to: a) the second amino acidic residue, Tyr107 (the nearest to the terminal amino group), and b) the His111 residue (pictures are shown in the Supporting Information). NMR results were able to shed light on this point. In fact, $k^{im}_{off}$ and $k^{bb}_{off}$ values obtained at pH 5.6 (see Table 8) allowed the $R_{1b}$ values reported in Table 9 to be calculated. These values were converted into $Cu^{II}$—H distances—also given in Table 9—by the following expression of the Solomon equation:[34]

$$R_{1b}=\frac{1}{10}\left(\frac{\mu_0}{4\pi}\right)^2\frac{\hbar\gamma_I^2\gamma_S^2}{r^6}\left\{\frac{\tau_c}{1+(\omega_I-\omega_S)^2\tau_c^2}+\frac{3\tau_c}{1+\omega_I^2\tau_c^2}+\frac{6\tau_c}{1+(\omega_I+\omega_S)^2\tau_c^2}\right\} \quad (3)$$

***Table 9.*** *Values of $R_{1b}$, and proton-copper distances (r) for the MLH complex: $r^{expt}$ = experimental (calculated from $R_{1b}$); $r^a_{mod}$ and $r^b_{mod}$ = calculated for the two structural hypotheses described in the text. The experimental distances are affected by an error of about 10%.*

| | $R_{1b}$ [$s^{-1}$] | $r^{expt}$ [nm] | $r^a_{mod}$ [nm] | $r^b_{mod}$ [nm] |
|---|---|---|---|---|
| $H_\alpha$ Lys106 | 6472 | 0.34 | 0.34 | 0.34 |
| $H_\alpha$ Thr107 | 71 | 0.72 | 0.39 | 0.60 |
| $H_\gamma$ Thr107 | 16 | 0.92 | 0.45 | 0.80 |
| $H_\beta$ Asn108 | 14 | 0.94 | 0.64 | 0.64 |
| $H_\varepsilon$ Met109 | 33 | 0.82 | 0.65 | 0.70 |
| $H_\beta$ His111 | 6472 | 0.34 | 0.40 | 0.32 |
| $H_\varepsilon$ Met112 | 14 | 0.94 | 1.20 | 1.00 |
| $H_\beta$ Ala113 | 6 | 1.07 | 1.20 | 1.10 |

A value of 0.22 ns was used for the correlation time ($\tau_c$), as calculated for the free peptide in solution by conventional methods.[35] In fact, since the dipolar interaction in the case of $Cu^{II}$ complexes with small ligands is exclusively modulated by reorientational dynamics, the motional correlation time of the free peptide is known to provide a very good approximation for $\tau_c$ in Equation (3).

The two models corresponding to the two isomers of MLH complex were subjected to geometry optimization with the HYPERCHEM program, and the obtained distances are also reported in Table 9. The agreement with experimental data is much better when the His111 (rather than Thr107) amide nitrogen is deprotonated and bound to copper (case b; Figure 7). It follows that the structure b is predominant at pH 5.6, even though the presence of small amounts of the second form cannot be excluded. It is worth noting that the further coordination of the carbonyl group belonging to the first (Lys106) residue, allowed by the complex stoichiometry, is not supported by any experimental evidence.

The main complex at physiological pH is the ML species (see Figures 1 and 2). The relevant shift in the VIS and EPR parameters, detected when the pH value is raised from 6 to 8, suggests the coordination to copper of a further amido nitrogen atom, as found in most $Cu^{II}$/peptide systems.[30] Both the corresponding $pK_{step}$ ($=\log\beta_{111}-\log\beta_{110}=6.6$) and $\Delta H^{\circ}_{step}$ ($\Delta H^{\circ}_{111}-\Delta H^{\circ}_{110}=-27\,kJ\,mol^{-1}$) values support this hypothesis. The same also holds true for the CD spectra, which show the expected blue shift in the d–d transition zone (see Supporting Information and Figure 3) without the onset of new absorption bands. As already pointed out for the MLH complex, different amido nitrogens could be involved in copper binding, thus leading to the formation of a number of isomeric complexes. The absence of NMR information at neutral pH did not allow direct evidence of the structure(s) of the existing complex(es) to be obtained. However it may be speculated that, at pH 7.4,

  

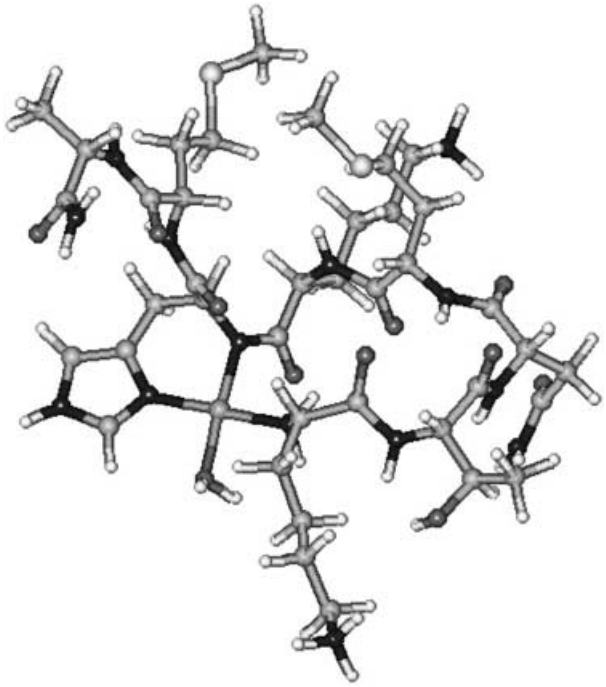

***Figure 7.*** *HYPERCHEM structure for the $Cu^{II}/PrP_{106-113}$ complex at pH 5.6.*

deprotonation and binding of Lys110 amide nitrogen occurs, as suggested by the observed $R_{1p}$ values (Figure 5). The resulting structural hypothesis for the ML species is shown in Figure 8. It is worth noting that this result agrees only partially with the previous spectroscopic[16] and X-ray[36] investigations into copper complexes of different PrP fragments at physiological pH. The

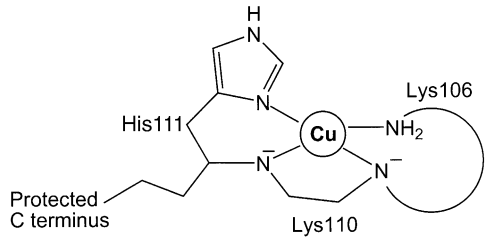


***Figure 8.*** *Structural hypothesis for the ML complex.*

data here confirm that the neurotoxic peptide $PrP_{106-126}$ binds the copper ion, and that its terminal amino and imidazolic group, along with some amido nitrogen of the peptidic chain, are involved in complex formation. However, no evidence was found of bis-complex formation or of participation of Met residues in complexation, at neutral pH.

If the pH value is raised, a new deprotonation step can be observed with the formation of the $MLH_{-1}$ complex, which dominates the alkaline pH range (see Figure 1 and Figure 2). This step is characterized by a $pK_{step}$ value of 8.3 – 8.6 (see Tables 3 and 5) and by a $\Delta H^{o}_{step}$ value of $-44\ kJ\,mol^{-1}$ (Table 3). The visible spectra clearly show a new "blue shift", while EPR data confirm a 4 N coordination in the equatorial plane.[23] The donor atom type should not change, as suggested by the corresponding CD spectrum, which is quite similar to that recorded at lower pH. This result allows us to exclude the participation of side amino groups of Lys residues in complexation. However, some important changes in the complex structure should take place between pH 8 and 9, given the remarkable shift recorded in the VIS spectra (shown in the Supporting Information). Moreover, NMR data at pH 9.0 show the appearance of relatively strong paramagnetic effects, almost equally spread over the backbone protons. Taking into account the structural hypotheses put forward above for the MLH and ML species, the experimental results on the $MLH_{-1}$ complex can be explained by the suggestion that a further amido nitrogen binds the copper ion in the equatorial plane of the complex, displacing the terminal amino group. The wavelength of maximum absorption registered in the VIS spectra at pH 9 (539 nm for both ligands) is lower than that expected[33] for a "pure" $\{3N^{-}, N_{Im}\}$ coordination (521 nm). This result could be attributable to an axial interaction of the terminal amino group with copper, which would just cause the observed "red shift".[33]

Finally, in the most alkaline pH range, the complex undergoes additional deprotonation steps which do not generate significant changes in the spectroscopic parameters. In the case of the $MLH_{-2}$ and $MLH_{-3}$ complexes, both the $pK_{step}$ and $\Delta H^{o}_{step}$ values almost exactly reproduce the values already found for Lys side chain deprotonation (Tables 1, 2, 3 and 5) in the absence of $Cu^{II}$ ions. This result supports the non-involvement of these groups in complex formation, over the whole pH range. The last complex species, appearing in solution at pH values higher than 10, should derive from the deprotonation of the unbound ("pyrrole-like") imidazole side chain nitrogen atom. The same deprotonation reaction, favoured by coordination of the other nitrogen atom to the metal ion, has already been observed,[32, 37] and the reported $pK_{step}$ values are in excellent agreement with those found in this investigation.

Finally, it is worth mentioning that the interaction between the $Cu^{II}$ ion and the sulfur atoms of Met residues at neutral pH has been suggested previously.[16, 36] This type of interaction should give rise to a charge-transfer absorption band, both in the visible and the CD spectra, around 450 nm,[38, 39] never observed in this study. NMR findings also exclude the involvement of sulfur atoms in metal binding, since i) no significant line-broadening corresponding to Met residues was detected after the addition of the paramagnetic ions and ii) the calculated $H_{\varepsilon}$ Met–$Cu^{II}$ distances are not consistent with $Cu^{II}$–S coordination. However, when a solution containing both the $Cu^{II}$ ion and one of the two ligands, at a pH value lower than 4.5, is frozen, it changes from colourless to yellow. At pH values higher than 4.5, on the other hand, the blue, violet or pink colour (depending on pH) of the solution is maintained in the frozen state. A similar observation in the case of a $Cu^{II}$/Met-containing dipeptide system was reported previously.[38] This yellow colour can be ascribed to the formation of some $Cu^{II}$–S bond: in fact, if the Met residues are replaced with *n*-leucine the yellow colour is not observed.[40] It is worth observing that sulfur is always in competition both with water molecules and the nitrogen-donor atoms of the ligand to bind the $Cu^{II}$ ion. At low pH, the nitrogens are protonated and cannot bind copper, while at pH values higher than 4.5 they are the preferential binding sites for the $Cu^{II}$

  

ions. Moreover, when the solution freezes, many water molecules most probably leave the hydration sphere of the metal ion to form structured ice clusters, thus allowing closer interaction between sulfur and copper. A full explanation of such phenomena will require further investigation.

## Experimental Section

**Materials**: The ligands, $PrP_{106-113}$ and $PrP_{106-126}$, were synthesized as described below. $Cu^{II}$ nitrate was an extra pure Merck product. The concentration of its stock solution was determined by ethylenediamine tetraacetate titration. The carbonate-free stock solution of KOH was prepared by diluting a saturated KOH (Aldrich, semiconductor grade) solution, under $N_2$ atmosphere, and then potentiometrically standardized by titrating known quantities of potassium hydrogen phthalate (Merck). The $HNO_3$ stock solution was prepared by diluting concentrated $HNO_3$ (Merck, Suprapur) and was then standardized with KOH. All sample solutions were prepared with freshly tetradistilled $CO_2$-free water. The ionic strength was adjusted to 0.1 M by addition of $KNO_3$ (Merck, Suprapur). Grade A glassware was employed throughout.

**Solid-phase peptide synthesis and purification**: The peptides were synthesized by published methods and standard solid-phase synthesis techniques[41] with a Milligen 9050 synthesizer. Protected amino acids and chemicals were purchased from Bachem, Novabiochem or Fluka (Switzerland). The resin, loaded with glycine (for $PrP_{106-126}$) or alanine (for $PrP_{106-113}$) on the polyethyleneglycol/polystyrene support (Fmoc-Xaa-PEG-PS; Xaa = Gly or Ala), was from Millipore (Waltham, MA, USA). $N^{\alpha}$-Fmoc derivatives of amino acids were used in the coupling reactions and all lateral amino acid protections were trifluoroacetic acid labile. Fmoc-Xaa-PEG-PS resin (1.0 g in all synthesis) was treated with piperidine (20%) in DMF and the $N^{\alpha}$-Fmoc amino acid derivatives (fourfold excess) were sequentially coupled to the growing peptide chain by use of [*O*-(7-azabenzotriazol-1-yl)-1,1,3,3-tetramethyluronium hexafluorophosphate] (HATU[42]; fourfold excess) in DMF, and the coupling reaction time was 1 h. Double coupling was required in the acylation steps of Leu and Val. Piperidine (20%) in DMF was used to remove the Fmoc group in all steps. After removal of the last $N^{\alpha}$-Fmoc group, the peptide resin was washed with methanol and dried in vacuo to yield the protected peptide-PEG-PS-resin. Protected peptides were cleaved from the resin by treatment with TFA/$H_2O$/phenol/ethanedithiol/thioanisole (reagent K; 82.5:5:5:2.5:5, *v/v*, 10 mL per 0.5 g of resin) at room temperature for 1 h.[43] After filtration of the exhausted resin, the solvent was concentrated in vacuo and the residue was triturated with ether. Crude peptides were purified by preparative reversed-phase HPLC with a Waters Delta Prep 4000 system and a Waters PrepLC 40 mm C18 assembly column (30 × 4 cm, 300 Å, 15 μm spherical particle size column). The column was perfused at a flow rate of 40 mL $min^{-1}$ with a mobile phase containing solvent A (water in 0.1% TFA), and a linear gradient from 10 to 60% of solvent B (acetonitrile in 0.1% TFA) over 25 min was adopted for the elution of the peptides. The pure fraction was collected to yield a white powder after lyophilization. Analytical HPLC analyses were performed on a Beckman 125 liquid chromatograph fitted with an Alltech C18 column (4.6 × 150 mm, 5 μm particle size) and equipped with a Beckman 168 diode array detector, with use of the above solvent system (solvents A and B) programmed at a flow rates of 1 mL $min^{-1}$, with a linear gradient from 0% to 50% or 0% to 80% B over 25 min. The molecular weights of the compounds were determined by MALDI-TOF analysis with a Hewlett Packard G2025A LD-TOF system mass spectrometer and α-cyano-4-hydroxycinnamic acid as a matrix.

**Potentiometric measurements**: Potentiometric titrations were performed with the following equipment: Orion EA 940 pH meter (resolution 0.1 mV, accuracy 0.2 mV) equipped with a combined glass electrode (Metrohm EA125); Hamilton MicroLab M motor burette (resolution 0.1 μL, accuracy 0.2 μL) equipped with a Hamilton syringe (delivery volume 500 μL). Both the potentiometer and the burette were interfaced with a personal computer; the titrations were automatically performed by use of a home-made program written in BASIC. Constant-speed magnetic stirring was applied throughout. The temperature of the titration cell was kept at 298.2 K by use of a Haake F3C circulation thermostat. UPP grade nitrogen, previously saturated with $H_2O$ (0.1 M $KNO_3$, 298.2 K) was blown over the test solution in order to maintain an inert atmosphere. The electrode couple was standardized on the $pH = -\log c_{H^+}$ scale by titration of $HNO_3$ (0.01 M) with standard KOH at 298.2 K and I = 0.1 M ($KNO_3$), before each titration. Aliquots (2 mL) of sample solution, containing suitable amounts of metal, ligand, $HNO_3$ and $KNO_3$, were titrated with standard KOH. The concentration range employed both for $Cu^{II}$ ion and for the ligands was 0.6 – 2.2 mM; the ligand/metal ratio was always slightly higher than 1:1.

**Calorimetric measurements**: Enthalpy values were determined by direct titration calorimetry with a Tronac model 450 isoperibol calorimeter with a 4 mL reaction vessel, at $T = 298.16 \pm 0.02$ K. The calorimetric measurements were carried out by titration in double aliquots of 2.5 mL of solutions of the same composition as above with standard $HNO_3$. The ionic strength was maintained constant at 0.1 M by addition of $KNO_3$. For each system at least 250 experimental points were utilized to calculate the thermodynamic quantities. The reaction heats, corrected for non-chemical contributions, which are of especial importance when small volume Dewars are used[44] and for the dilution heats computed from literature data,[45] were calculated by considering the calorie as equivalent to 4.184 J.

**Spectroscopic measurements**: The absorption spectra were recorded with a Uvicon 931 (Kontron) spectrophotometer with a glass cell (W110/S4, 1 cm pathlength); the temperature was maintained at 298 K by use of a Kontron GTD-900 circulation thermostat. Circular dichroism (CD) spectra were recorded on a Jasco J715 spectropolarimeter. EPR spectra were recorded on a Bruker ESP 300E (at 120 K and 9.5 GHz). Sample solutions had the same composition as above; pH was varied by addition of suitable amounts of standard NaOH or HCl, under potentiometric control. Spectra were recorded every 0.5 pH units. NMR spectra were performed at 14.1 T with a Bruker Avance 600 MHz spectrometer at controlled temperatures (±0.1 K). Two different peptide solutions were prepared: the first with deionized water containing 10% $D_2O$, the second with deuterium oxide (99.95% from Merck), and they were carefully deoxygenated by a freezing/vacuum pumping/sealing/thawing procedure. The pH was adjusted to desired values with either DCl or NaOD. The desired concentration of copper ions was achieved by use of a stock solution of copper nitrate (Sigma) in deuterium oxide. [$D_4$]TSP (3-(trimethylsilyl)-[2,2,3,3-$d_4$] propanesulfonate) sodium salt, was used as internal reference standard. Suppression of residual water signal was achieved by excitation sculpting[46] by use of a 2 ms long selective square pulse on water. A typical NMR spectrum required 16 transients acquired with a 9.1 μs 90° pulse, 6600 Hz spectral width, and 2.0 s recycling delay. The assignment was accomplished with TOCSY, COSY, NOESY and ROESY 2D experiments. TOCSY spectra were recorded with a total spin-locking time of 75 ms by use of a MLEV-17 mixing sequence. Rotating frame Overhauser enhancement spectroscopy (ROESY) was performed at a mixing time of 300 ms and the radio frequency strength for the spin-lock field was 1.9 KHz. The

  

spectral width of homonuclear 2D experiments was typically 6000 Hz in both $F_1$ and $F_2$ dimensions. Spin–lattice relaxation rates were measured with inversion recovery pulse sequences. The same sequence was also used to measure the single-selective relaxation rates by use of suitably shaped $\pi$ pulses instead of the usual non-selective $\pi$ pulse. All rates were calculated by regression analysis of the initial recovery curves of longitudinal magnetization components leading to errors not larger than $\pm 3\%$.

**Calculations**: The potentiometric data processing, concerning both the standardization of the electrode system and the calculation of protonation/complex formation constants, was performed by use of the least-squares computer program SUPERQUAD.[47] The complex species are reported throughout as $M_pL_qH_r$, referring to the overall equilibrium.

$$pM + qL + rH = M_pL_qH_r \quad (4)$$

Here M is the metal, L the ligand, and H the proton. Charges are omitted for the sake of simplicity. The corresponding overall equilibrium constants are indicated as $\beta_{pqr}$. To obtain the species distribution the computer program HYSS[48] was used. $\Delta H^\circ_{pqr}$ values were computed from the experimental calorimetric titrations by use of the computer program DOEC.[49] The corresponding $\Delta S^\circ_{pqr}$ values were computed from the Gibbs–Helmholtz equation.

$$-\Delta G^\circ_{pqr} = -\Delta H^\circ_{pqr} + T\Delta S^\circ_{pqr} \quad (5)$$

Here the free energy variation was given by potentiometry: $-\Delta G^\circ_{pqr} = 2.303\,RT\log\beta_{pqr}$. A $pK_w$ value of 13.74 and a $\Delta H^\circ_w$ value of 55.9 kJ mol$^{-1}$,[50] checked by separate experiments, were employed in the calculations. The precision of each thermodynamic parameter is reported throughout as the standard deviation given by the corresponding least squares program and it is shown in parentheses as uncertainty on the last significant figure. Molecular structures were generated by use of the HYPERCHEM software package[51] implemented on a Pentium III PC by use of the ZINDO-1 semi-empirical method for charge calculations and the MM+ force-field for molecular mechanics and dynamics calculations.

## Acknowledgements

*Financial support by the University of Ferrara (ex-60%), the Polish State Committee for Scientific Research (KBN 4 T09A 054 23) and MURST COFIN 2001 is gratefully acknowledged. Many of the 600 MHz spectra were recorded at the SON NMR Large Scale Facility in Utrecht, which is funded by the "Access to Research Infrastructures" program of the European Union (HPRI-CT-1999-00005 or HPRI-CT-2001-00172). We also thank Dr. Raffaele Lamanna (ENEA CRTRISAIA) and Dr. Anna Laura Segre (CNR Montelibretti Rome) for their skilful technical assistance in NMR spectroscopy and for helpful discussion.*

**Keywords:** bioinorganic chemistry · complexes · copper · peptides · prion proteins

[1] S. B. Prusiner, *Proc. Natl. Acad. Sci. USA* **1998**, *95*, 13 363 – 13 383.
[2] S. B. Prusiner, *N. Engl. J. Med.* **2001**, *20*, 1516 – 1526.
[3] V. M. Martins, R. Linden, M. A. M. Prado, R. Walz, A. C. Sakamoto, I. Izquierdo, R. R. Brentani, *FEBS Lett.* **2002**, *512*, 25 – 28.
[4] D. R. Brown, K. Qin, J. W. Herms, A. Madlung, J. Manson, R. Strome, P. E. Fraser, T. A. Kruck, A. von Bohlen, W. Schulz-Schaeffer, A. Giese, D. Westaway, H. Kretzschmar, *Nature* **1997**, *390*, 684 – 687.
[5] D. R. Brown, J. Sassoon, *Mol. Biotechnol.* **2002**, *22*, 165 – 178.
[6] S. Lehmann, *Curr. Opin. Chem. Biol.* **2002**, *6*, 187 – 192.
[7] D. J. Waggoner, T. B. Bartnikas, J. D. Gitlin, *Neurobiol. Dis.* **1999**, *6*, 221 – 230.
[8] C. S. Burns, E. Aronoff-Spencer, G. Legname, S. B. Prusiner, W. E. Antholine, G. J. Gerfen, J. Peisach, G. L. Millhauser, *Biochemistry* **2003**, *42*, 6794 – 6803, and references therein.
[9] G. Forloni, N. Argeretti, R. Chiesa, E. Monzani, M. Salmona, O. Bugiani, F. Tagliavini, *Nature* **1993**, *362*, 543 – 546.
[10] C. Selvaggini, L. De Gioia, L. Cantû, E. Ghibaudi, L. Diomede, F. Passerini, G. Forloni, O. Bugiani, F. Tagliavini, M. Salmona, *Biochem. Biophys. Res. Commun.* **1993**, *194*, 1380 – 1386.
[11] M. Ettaiche, R. Pichot, J.-P. Vincent, J. Chabry, *J. Biol. Chem.* **2000**, *275*, 36 487 – 36 490.
[12] D. R. Brown, J. Herms, H. A. Kretzschmar, *NeuroReport* **1994**, *5*, 2057 – 2060.
[13] D. R. Brown, *Biochem. J.* **2000**, *352*, 511 – 518.
[14] a) V. Meske, F. Albert, T. G. Ohm, *Acta Neuropathol.* **2002**, *104*, 560 – 560; b) M. Perez, A. I. Rojo, F. Wandosell, J. Diaz-Nido, J. Avila, *Biochem. J.* **2003**, *372*, 129 – 136; c) J. I. Kourie, B. L. Kenna, D. Tew, M. F. Jobling, C. C. Curtain, C. L. Masters, K. J. Barnham, R. Cappai, *J. Membrane Biol.* **2003**, *193*, 35 – 45; d) N. C. Kaneider, A. Kaser, S. Dunzendorfer, H. Tilg, C. J. Wiedermann, *J. Virol.* **2003**, *77*, 5535 – 5539; e) T. Florio, D. Paludi, V. Villa, D. R. Principe, A. Corsaro, E. Millo, G. Damonte, C. D'Arrigo, C. Russo, G. Schettini, A. Aceto, *J. Neurochem.* **2003**, *85*, 62 – 72; f) N. Numao, N. Noguchi, Y. Eguchi, S. Watanabe, T. Fukui, T. Kamino, N. Shimozono, A. Yamazaki, S. Kobayashi, M. Sasatsu, *Biol. Pharm. Bull.* **2003**, *26*, 229 – 232.
[15] C. S. Atwood, R. D. Moir, X. Huang, R. C. Scarpa, N. M. E. Bacarra, D. M. Romano, M. A. Hartshorn, R. E. Tanzi, A. I. Bush, *J. Biol. Chem.* **1998**, *273*, 12 817 – 12 826.
[16] M. F. Jobling, X. Huang, L. R. Stewart, K. J. Barnham, C. Curtain, I. Volitakis, M. Perugini, A. R. White, R. A. Cherny, C. L. Masters, C. J. Barrow, S. J. Collins, A. I. Bush, R. Cappai, *Biochemistry* **2001**, *40*, 8073 – 8084.
[17] D. R. Brown, B. Schmidt, H. A. Kretzschmar, *Nature* **1996**, *380*, 345 – 347.
[18] S. Turnbull, B. J. Tabner, D. R. Brown, D. Allsop, *Neurosci. Lett.* **2003**, *336*, 159 – 162.
[19] M. F. Jobling, L. R. Stewart, A. R. White, C. McLean, A. Friedhuber, F. Maher, K. Beyreuther, C. L. Masters, C. J. Barrow, S. J. Collins, R Cappai, *J. Neurochem.* **1999**, *73*, 1557 – 1565.
[20] C. Conato, W. Kamysz, H. Kozłowski, M. Luczkowski, Z. Mackiewicz, F. Mancini, P. Mlynarz, M. Remelli, D. Valensin, G. Valensin, *Eur. J. Inorg. Chem.* **2003**, 1694 – 1702.
[21] L. D. Pettit, H. K. J. Powell, *The IUPAC Stability Constants Database*, Academic Software and IUPAC, Royal Society of Chemistry, London, **1992 – 2000**.
[22] P. G. Daniele, E. Prenesti, G. Ostacoli, *J. Chem. Soc. Dalton Trans.* **1996**, 3269 – 3275.
[23] J. Peisach, W. E. Blumberg, *Arch. Biochem. Biophys.* **1974**, *165*, 691 – 708.
[24] R. S. Molday, S. W. Englander, R. G. Gallen, *Biochemistry* **1972**, *11*, 150 – 158.
[25] Y. Bai, J. S. Milne, L. Mayne, S. W. Englander, *Proteins Struct. Funct. Genet* **1993**, *17*, 75 – 86.
[26] C. Conato, W. Kamysz, H. Kozłowski, M. Luczkowski, Z. Mackiewicz, P. Mlynarz, M. Remelli, D. Valensin, G. Valensin, *J. Chem. Soc. Dalton Trans.* **2002**, 3939 – 3944.
[27] M. Luczkowski, H. Kozłowski, M. Stawikowski, K. Rolka, E. Gaggelli, D. Valensin, G. Valensin, *J. Chem. Soc. Dalton Trans.* **2002**, 2269 – 2274, and references therein.
[28] I. Bertini, C. Luchinat, *Coord. Chem. Rev.* **1996**,*150*, 1 – 296.
[29] E. Gaggelli, N. D'Amelio, D. Valensin, G. Valensin, *Magn. Resonan. Chem.* **2003**, *41*, 877 – 883.
[30] L. D. Pettit, J. E. Gregor, H. Kozłowski in *Perspectives on Bioinorganic Chemistry, Vol. 1* (Eds.: R. W. Hay, J. R. Dilworth, K. B. Nolan), JAI Press, London, **1991**, pp. 1 – 41.
[31] G. Borghesani, F. Pulidori, M. Remelli, R. Purrello, E. Rizzarelli, *J. Chem. Soc. Dalton Trans.* **1990**, 2095 – 2100.
[32] M. Remelli, M. Luczkowski, A. M. Bonna, Z. Mackiewicz, C. Conato, H. Kozłowski, *New J. Chem.* **2003**, *27*, 245 – 250.
[33] H. Sigel, R. B. Martin, *Chem. Rev.* **1982**, *82*, 385 – 426.

  

[34] I. Solomon, *Phys. Rev.* **1955**, *99*, 559 – 565.
[35] R. Freeman, H. D. W. Hill, L. D. Hall, B. L. Tomlinson, *J. Chem. Phys.* **1974**, *61*, 4466 – 4473.
[36] S. S. Hasnain, L. M. Murphy, R. W. Strange, J. G. Grossmann, A. R. Clarke, J. S. Jackson, J. Collinge, *J. Mol. Biol.* **2001**, *311*, 467 – 473.
[37] P. Młynarz, D. Valensin, K. Kociolek, J. Zabrocki, J. Olejnik, H. Kozłowski, *New J. Chem.* **2002**, *26*, 264 – 268.
[38] H. Kozłowski, T. Kowalik, *Inorg. Nucl. Chem. Lett.* **1978**, *14*, 201 – 205.
[39] H. Kozłowski, T. Kowalik, *Inorg. Chim. Acta* **1979**, *34*, L231 – L233.
[40] B. Belosi, R. Guerrini, H. Kozłowski, M. Łuczkowski, M. Remelli, unpublished preliminary results.
[41] E. Atherton, R. C. Sheppard in *Solid Phase Peptide Synthesis* (Eds: D. Rickwood, B. D. Hames), IRL Press, Oxford, **1989**.
[42] 1-Hydroxy-7-azabenzotriazole. An efficient peptide coupling additive. L. A. Carpino, *J. Am. Chem. Soc.* **1993**, *115*, 4397 – 4398.
[43] A cleavage method minimizing side reactions following Fmoc solid-phase peptide synthesis. D. S. King, C. G. Fields, G. B. Fields, *Int. J. Pept. Protein Res.* **1990**, *36*, 255 – 266.
[44] L. D. Hansen, T. E. Jensen, S. Mayne, D. J. Eatough, R. M. Izatt, J. J. Christensen, *J. Chem. Thermodynamics* **1975**, *7*, 919 – 926.
[45] V. B. Parker, *Thermal Properties of Aqueous Uni-Univalent Electrolytes*, Natl. Stand. Ref. Data Ser. NBS (US) 2, US Government Printing Office, Washington, **1965**.
[46] T. L. Hwang, A. J. Shaka, *J. Magn. Reson. Series A* **1995**, *112*, 275 – 279.
[47] P. Gans, A. Sabatini, A. Vacca, *J. Chem. Soc. Dalton Trans.* **1985**, 1195 – 1200.
[48] L. Alderighi, P. Gans, A. Ienco, D. Peters, A. Sabatini, A. Vacca, *Coord. Chem. Rev.* **1999**, *184*, 311 – 318.
[49] C. Rigano, E. Rizzarelli, S. Sammartano, *Thermochim. Acta* **1979**, *33*, 211 – 216.
[50] A. Sabatini, A. Vacca, L. Bologni, *J. Chem. Soc. Dalton Trans.* **1981**, 1246 – 1250.
[51] *HYPERCHEM*, *Hypercube release 5.1 Pro for Windows*, Hypercube Inc., Waterloo, Canada, **1997**.

Received: October 13, 2003 [F 786]

  